JOURNAL OF Materials CHEMISTRY

Oxygen ion transport in La_2NiO_4-based ceramics

Vladislav V. Kharton,*†[a] Alexandre P. Viskup,[a] Eugene N. Naumovich[a] and Fernando M. B. Marques[b]

[a]*Institute of Physicochemical Problems, Belarus State University, 14 Leningradskaya Str., 220080 Minsk, Republic of Belarus*
[b]*Ceramics and Glass Engineering Department, University of Aveiro, 3810 Aveiro, Portugal*

Received 26th April 1999, Accepted 15th July 1999

The solid solutions $La_2Ni_{1-x}Fe_xO_{4+\delta}$ ($x=0.02$ and 0.10), $La_{1.9}Sr_{0.1}Ni_{1-x}Fe_xO_{4+\delta}$ ($x=0.02$ and 0.10) and $La_2Ni_{0.88}Fe_{0.02}Cu_{0.10}O_{4+\delta}$ with the tetragonal K_2NiF_4-type structure were prepared by a standard ceramic technique. The thermal expansion coefficients of the ceramic materials, calculated from dilatometric data, are in the range $(10.5–13.2)\times10^{-6}$ K^{-1} at 300–1100 K. Oxygen permeation fluxes through dense $La_2NiO_{4+\delta}$-based membranes at 970–1170 K were found to be limited by both surface exchange and bulk ionic transport, whereas the limiting effect of the oxygen interphase exchange increases with decreasing oxygen pressure at the membrane permeate side and with decreasing temperature. Applying porous cermet layers of dispersed platinum and praseodymium oxide onto the membrane surface results in enhanced permeation fluxes. The maximum oxygen permeability was found for the $La_2Ni_{0.98}Fe_{0.02}O_{4+\delta}$ and $La_2Ni_{0.88}Fe_{0.02}Cu_{0.10}O_{4+\delta}$ solid solutions; oxygen permeability data demonstrated that a vacancy diffusion mechanism and oxygen interstitial migration make significant contributions to the total ionic conductivity.

Introduction

Developing novel oxide materials with high mixed ionic–electronic conductivity is of considerable interest for numerous applications such as solid oxide fuel cells (SOFCs), high temperature gas electrolyzers, sensors, ceramic membranes for high-purity oxygen separation and partial oxidation of hydrocarbons.[1–6] Using mixed conductors as electrode materials for SOFCs and other solid electrolyte cells leads, as a rule, to decreasing polarization losses due to an enlargement of the electrochemical reaction zone.[1] Technologies for hydrocarbon oxidation using ceramic mixed-conductive membranes permit the integration of oxygen separation, steam reforming and partial oxidation into a single step for natural gas conversion.[3,4] In addition, the presence of active oxygen species (O_2^-, O^-) at the membrane surface may improve the selectivity of hydrocarbon oxidation reactions. This work is focused on the transport properties of ceramic materials based on lanthanum nickelate, $La_2NiO_{4+\delta}$, substituted in both cation sublattices.

The crystal lattice of lanthanum nickelate is related to the K_2NiF_4-type and can be described as a succession of perovskite layers alternating with rock salt LaO layers.[7,8] $La_2NiO_{4+\delta}$ has been shown to exhibit a wide range of oxygen hyperstoichiometry ($0\leqslant\delta\leqslant0.25$), which determines the phase composition, structure and the transport and magnetic properties.[7–11] Oxygen excess in $La_2NiO_{4+\delta}$ is associated with the incorporation of interstitial oxygen anions into the rock salt layers. As for $La_2CuO_{4+\delta}$,[12] the lanthanum nickelate phase does not exist in the hypostoichiometric region when $\delta<0$.[13] The equilibrium oxygen nonstoichiometry in air was determined to be close to 0.14 at room temperature and to decrease with increasing temperature down to 0.04.[10,11,13,14] Under these conditions, $La_2NiO_{4+\delta}$ forms a tetragonal phase (space group *I*4/*mmm*).[9–11] Incorporation of strontium into the lanthanum sublattice of $La_{2-x}Sr_xNiO_{4\pm\delta}$ solid solutions leads to decreasing oxygen content; however, all oxides with $x\leqslant0.5$ are hyperstoichiometric in the temperature range 300–1320 K.[13]

At temperatures below approximately 600 K, lanthanum nickelate exhibits a semiconductor-type electronic conductivity which probably occurs by hopping of p-type charge carriers between mixed valence nickel cations.[7,8,13] When the temperature increases, a transition from semiconducting to metal-like behaviour is observed; the values of electronic conductivity for $La_2NiO_{4+\delta}$ at 600–1100 K in air were reported to vary from approximately 10 to 100 S cm^{-1}.[13,15,16] Substitution of strontium for lanthanum results in an increase in conductivity of the $La_{2-x}Sr_xNiO_{4\pm\delta}$ solid solutions at moderate dopant concentrations ($0\leqslant x\leqslant0.6$).[7,13,16] Doping $LaSrNiO_{4-\delta}$ with iron has the the reverse effect, probably due to the stable oxidation state of Fe^{3+} cations in comparison with nickel ions.[17] Estimations of the oxygen chemical diffusion coefficients, obtained by coulometric titration and electrochemical oxidation methods,[18,19] indicated that the mobility of oxygen ions in lanthanum–strontium nickelates is particularly high. For instance, the chemical diffusion coefficient, estimated from data on the electrochemical oxidation of $La_2NiO_{4+\delta}$ in aqueous KOH at room temperature, and averaged in the range of $0.06\leqslant\delta\leqslant0.145$, was found to be as high as about 10^{-7} cm^2 s^{-1}.[18] It should be noted that the chemical diffusion coefficients obtained from the results of such experiments are apparently much higher than those calculated from extrapolation of high temperature diffusion coefficients.[18] Values of the oxygen chemical diffusion coefficient in $La_{1.8}Sr_{0.2}NiO_{4+\delta}$, calculated from coulometric titration results at 770–1320 K under an oxygen partial pressure of 1–285 Pa, vary from approximately 7×10^{-7} to 1×10^{-5} cm^2 s^{-1} and decrease with decreasing oxygen pressure.[19] K_2NiF_4-type phases based on lanthanum nickelate were thus reported to possess relatively high values of both electronic and ionic conductivities, which makes significant oxygen permeability likely.[13] However, the mechanism of oxygen transport in nickelates is not yet clear.

Experimental

Synthesis of $La_2Ni_{1-x}Fe_xO_{4+\delta}$ ($x=0.02$ and 0.10), $La_{1.9}Sr_{0.1}Ni_{1-x}Fe_xO_{4+\delta}$ ($x=0.02$ and 0.10) and

†Present address: Ceramics and Glass Engineering Department, University of Aveiro, 3810 Aveiro, Portugal. E-mail: kharton@cv.ua.pt

Table 1 List of abbreviations

Composition	Abbreviation
$La_2Ni_{0.98}Fe_{0.02}O_{4+\delta}$	LNF2
$La_2Ni_{0.90}Fe_{0.10}O_{4+\delta}$	LNF10
$La_{1.90}Sr_{0.10}Ni_{0.98}Fe_{0.02}O_{4+\delta}$	LSNF2
$La_{1.90}Sr_{0.10}Ni_{0.90}Fe_{0.10}O_{4+\delta}$	LSNF10
$La_2Ni_{0.88}Fe_{0.02}Cu_{0.10}O_{4+\delta}$	LNF2CU10

$La_2Ni_{0.88}Fe_{0.02}Cu_{0.10}O_{4+\delta}$ was carried out by a standard ceramic technique. Henceforth, ceramic compositions under study are designated by abbreviations such as LNF2 or LSNF10; a list of abbreviations is given in Table 1. High purity $La(NO_3)_3{\cdot}6H_2O$, $SrCO_3$, $Ni(HCOO)_2{\cdot}2H_2O$, CuC_2O_4 and $FeC_2O_4{\cdot}2H_2O$ were used as starting materials. The starting mixtures were initially dissolved in an aqueous solution of nitric acid, dried and then thermally decomposed. The solid-state reactions were conducted in air at temperatures of 1270 to 1520 K for 15–30 h with multiple intermediate grinding steps. Ceramic specimens were pressed (300–450 MPa) into bars ($4\times4\times30$ mm^3) and disks of various thickness (diameter 12 or 15 mm). Gas-tight ceramics were sintered in air at 1750–1890 K over 10–15 h. After sintering, the specimens were annealed in air at 1170 K for 6–15 hours, slowly cooled and then kept at room temperature in air for a period of 30–90 days in order to obtain oxygen nonstoichiometry values as close as possible to the equilibrium values. The density of the ceramics was greater than 92% of the theoretical density calculated from X-ray diffraction (XRD) data.

The prepared powders and ceramics were characterized by XRD, X-ray fluorescence analysis (XFA), thermal gravimetric analysis (TGA), emission spectroscopic analysis, scanning electron microscopy (SEM) and dilatometry. The characterization techniques, methods for testing gas tightness and details on measuring electrical conductivity are described elsewhere.[20–24] The oxygen nonstoichiometry values were calculated from the results of TGA of the powders which had been heated in air up to 1070 K and then reduced in a hydrogen flow at 1170–1270 K.

Only specimens which had been verified as gas tight were used for oxygen permeability measurements. The technique used to determine stationary oxygen permeation fluxes, using yttria-stabilized zirconia (YSZ) solid-electrolyte cells equipped with an electrochemical oxygen pump and a sensor, has been described in detail elsewhere.[20–22] The cells consisted of three separate parts: an oxygen pump, a sensor and a YSZ ring which separated the pump and sensor; each part was fabricated independently and then sealed into a single cell. This construction was chosen in order to prevent the voltage applied to the electrodes of the oxygen pump affecting the sensor e.m.f. reading; this was checked after assembling the cells. The cells were also checked for gas leakages by sealing another oxygen pump onto the cells and simulating known oxygen permeation fluxes. The total oxygen leakage currents did not exceed 10 μA, which is less than 0.2% of the measured permeation fluxes. In addition, the accuracy of the permeation flux measurements was verified using two independent experimental set-ups.[21,23] In the first of these techniques, the oxygen permeation fluxes which passed through the membrane were fed into a measurement device evacuated by a vacuum pump, described in detail in ref. 21. The second method involved passing an inert sweep gas over the membrane and then determining its oxygen concentration.[23]

Oxygen permeability was measured at temperatures from 950 to 1250 K with a difference in oxygen partial pressure at the membrane sides between 2×10^4 and 1×10^3 Pa. For all the results presented in this paper, oxygen pressure at the membrane feed side (p_2) was maintained at 0.21×10^5 Pa (atmospheric air). The time required to achieve a steady state in the cell ranged from 3 to 100 h.

For further analysis of the oxygen permeation processes we will use the oxygen permeation flux density j (mol s^{-1} cm^{-2}) and the specific oxygen permeability $J(O_2)$ (mol s^{-1} cm^{-1}), which are related by the equation:[25]

$$J(O_2) = jd[\ln(p_2/p_1)]^{-1} \quad (1)$$

where d is the thickness of the measured specimen and p_1 is the oxygen partial pressure at the membrane permeate side ($p_2>p_1$). The ceramic membrane thickness was varied from 0.50 to 1.50 mm.

The quantity $J(O_2)$ is convenient for the identification of the limiting effect of the surface exchange rate on the oxygen permeation, on the basis of the thickness dependence of the permeation flux.[20–22] As the oxygen permeability is proportional to $j\times d$ by definition, $J(O_2)$ should be independent of thickness if surface limitations on the oxygen permeation flux are negligible. In this case, the physical meaning of the oxygen permeability quantity refers to the ambipolar conductivity (σ_{amb}) of the membrane material, averaged for a given oxygen partial pressure range:

$$J(O_2) = \frac{RT}{16F}\,\overline{\sigma_{amb}} = \frac{RT}{16F}\,\frac{\overline{\sigma_o\sigma_e}}{\sigma_o+\sigma_e} \quad (2)$$

where σ_o and σ_e are the oxygen ionic and electronic conductivities, respectively. The electronic conductivity of the $La_2NiO_{4+\delta}$-based solid solutions is much higher than the ionic conductivity ($\sigma_o\ll\sigma_e$), and the specific oxygen permeability is expected to be proportional to the averaged oxygen conductivity within the membrane thickness range where no thickness dependence of $J(O_2)$ is observed:

$$J(O_2) \approx \frac{RT}{16F}\,\overline{\sigma_o} \quad (3)$$

In the case where interphase oxygen exchange limitations are considerable, $J(O_2)$ should increase with increasing membrane thickness due to the reduced influence of the surface exchange rate for a given oxygen chemical potential gradient.

It should be noted that both the ionic conductivity and exchange currents of perovskite-related oxides are functions of oxygen chemical potential (see, for example, ref. 3,6,19,22,23). The values of $J(O_2)$ are presented here, therefore, in combination with the corresponding values of p_1 and p_2.

Results and discussion

Structure and oxygen nonstoichiometry

XRD results demonstrated that all the ceramic samples were single phase; only reflections due to the tetragonal K_2NiF_4-type phase, characteristic for $La_2NiO_{4+\delta}$ in air, were observed in the XRD patterns; the tetragonal unit cell parameters (a and c) of the solid solutions are given in Table 2. Table 2 also lists the values of oxygen hyperstoichiometry, δ, and its reproducibility error. One should note that increasing iron concentration resulted in poorer reproducibility of TGA data under reduction and excessively long equilibration times. For LNF10, the extremely poor reproducibility of the oxygen nonstoichimetry data may also have been because the composition of the oxide is close to the single phase stability limits. As a result, the hyperstoichimetry of LNF10 at room temperature was only able to be estimated to exceed 0.20.

According to the XRD data, incorporation of strontium into the lanthanum sublattice results in a decreasing a and an increasing c parameter. The effect on the crystal lattice of substituting copper for nickel is analogous, but the variation in the a values for LNF2 and LNF2CU10 in this case is within the limits of experimental error. Here, oxygen content in the oxides

Table 2 Properties of the $La_2NiO_{4+\delta}$-based ceramics

	Unit cell parameters		Oxygen nonstoichiometry in air, δ		
Abbreviation	*a*/nm	*c*/nm	300 K	1073 K	$10^6\ \bar{\alpha}/K^{-1}$
LNF2	0.3864	1.2661	0.151 ± 0.007	—	13.2 ± 0.2
LNF10	0.3872	1.2673	—	—	12.8 ± 0.3
LSNF2	0.3855	1.2682	0.108 ± 0.007	0.04 ± 0.01	12.5 ± 0.1
LSNF10	0.3869	1.2685	0.148 ± 0.007	0.08 ± 0.01	12.7 ± 0.3
LNF2CU10	0.3866	1.2691	0.138 ± 0.005	0.083 ± 0.005	10.5 ± 0.2

$\bar{\alpha}$ is the thermal expansion coefficient calculated from the dilatometric data and averaged over the temperature range 300–1100 K.

decreased on doping with either strontium or copper. These results are in excellent agreement with literature data on the $La_{2-x}Sr_xNiO_{4\pm\delta}$[7,13] and $La_2Ni_{1-x}Cu_xO_{4+\delta}$[26] solid solutions.

When iron cations are introduced into the nickel sublattice, both the *a* and *c* parameters tend to increase with iron content (Table 2). Taking into account literature data,[9,10] one can assume that such behaviour is associated with increasing oxygen hyperstoichiometry. An increase in oxygen content on doping with higher-valence cations is characteristic of perovskite-like oxides. For instance, an increase in the oxygen hyperstoichimetry with *x* was observed for the $La_2Cu_{1-x}Co_xO_{4+\delta}$ solid solutions.[27] Similarly, doping $Bi_2CuO_{4\pm\delta}$ with nickel, which has a higher average oxidation state than copper, results in increasing oxygen content.[28] In the case of undoped $La_2NiO_{4+\delta,}$ increasing δ was established to lead to a transition of the tetragonal (*I*4/*mmm*) phase to orthorhombic symmetry (*Fmmm*);[9,10] both the basal plane lattice constants (*a* and *b*) and the *c* parameter of the orthorhombic phase increase with δ.[9]

Electrical conductivity and thermal expansion

The results of electrical conductivity measurements performed with the $La_2NiO_{2+\delta}$-based solid solutions (Fig. 1) are also in good agreement with the literature data.[7,13,15–17,26] For all the compounds studied, a transition from semiconductor-like to metallic conductivity was observed in the temperature range 600–770 K. The electronic conductivity of the oxides increases on doping with strontium, and decreases slightly when nickel cations are substituted by copper ions. The physical nature of such behavior has been discussed in detail in numerous research articles.[7,15–17,26] Moderate addition of iron leads to increasing conductivity in Fe-doped lanthanum nickelate, which indicates that iron cations may contribute to the electronic transport. However, the conductivity in Sr-containing solid solutions was found to decrease with increasing iron concentration (compare curves 3 and 4 in Fig. 1). Most probably, simultaneous doping of lanthanum nickelate by iron and strontium results in a stabilization of the Fe^{3+} oxidation state, typical for the $LaSrFeO_{4+\delta}$ phase, thus decreasing the concentration of the B-site cations which contribute to electron conduction. This assumption is supported by data on the electrical conductivity at temperatures below 500 K, when the conductivity of LNF10 ceramics exceeds that of LSNF10 by a factor of 1.1–1.5. It is obvious, however, that more detailed studies are necessary to clarify the observed phenomena.

Table 2 lists thermal expansion coefficients (TECs) of the studied ceramics in air, obtained by linear regression analysis of the dilatometric data within the temperature range 300–1100 K. TECs varied in the range $(10.5–13.2) \times 10^{-6}\ K^{-1}$, decreasing slightly with increasing dopant content; these TEC values are close to those of the $La_{2-x}Sr_xNiO_{2+\delta}$ solid solutions reported in ref. 29.

Surface limitation of oxygen permeation fluxes

Oxygen permeation fluxes through the title materials as a function of oxygen chemical potential difference, membrane thickness and temperature are given in Fig. 2. Fig. 3 presents the corresponding values of the oxygen permeability calculated from eqn. (1). For all the materials under study, the $J(O_2)$ values increased with membrane thickness, whilst oxygen permeation fluxes decreased regularly with increasing *d*. This shows unambiguously that oxygen transport through nickelate ceramics is limited by both bulk ionic conductivity and surface exchange rate. Such behaviour is similar to that of the $La_2Cu_{1-x}Co_xO_{4+\delta}$ solid solutions reported in one of our previous works.[27] The results given in Fig. 3 also show that the limiting effect of the surface exchange on the permeation flux increases with increasing oxygen chemical potential gradient. Indeed, the values of the oxygen permeability for membranes with different thicknesses were determined to be close to each other in the range $0.07 < p_1 < 0.21$ atm. Further reduction of the oxygen pressure at the membrane permeate side leads to an increasing difference in the $J(O_2)$ values. Decreasing temperature also results in a greater limiting effect of the oxygen interphase exchange.

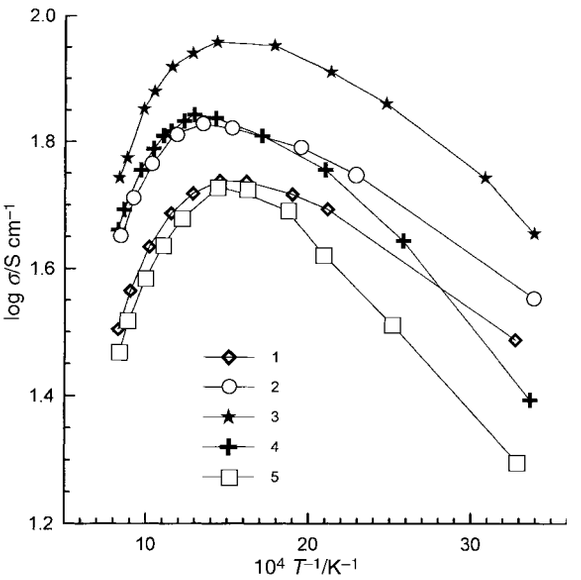

Fig. 1 Temperature dependence of the electrical conductivity in air: (1), LNF2; (2), LNF10; (3), LSNF2; (4), LSNF10; (5), LNF2CU10.

Further evidence regarding the increasing role of the surface exchange limitations with increasing oxygen pressure gradients was obtained by studying the LNF10 membrane with an activated feed-side surface. For the surface modification, highly dispersed platinum with added praseodymium oxide (about 30 wt%) was used. Praseodymium oxide is known to possess a high electrocatalytic activity in electrochemical reactions involving oxygen.[30,31] Such additions were thus expected to enhance the catalytic activity of the membrane surface. A porous layer consisting of a mixture of dispersed platinum and Pr_6O_{11} with a layer density of approximately 10 mg cm^{-2} was deposited onto the feed-side surface of the LNF10 ceramic disk; the disk was then annealed at 1270 K for 2 h. For

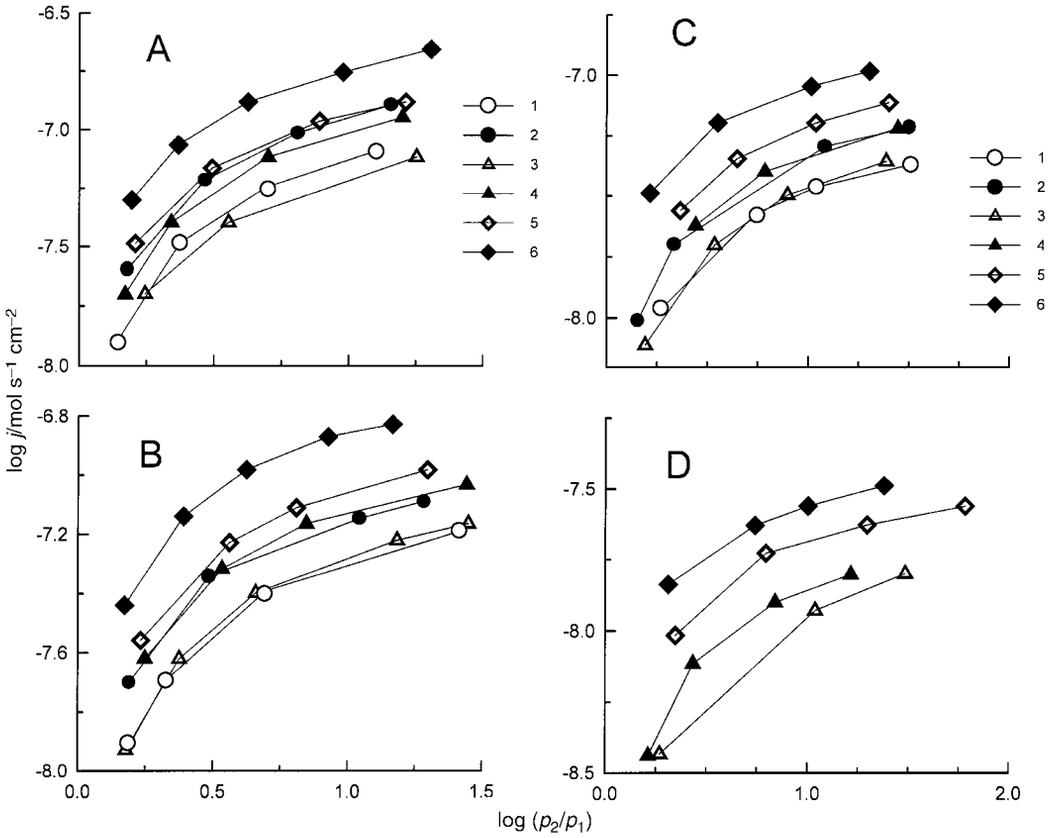

Fig. 2 Dependence of the oxygen permeation flux density on the oxygen partial pressure gradient at: A, 1173 K; B, 1123 K; C, 1073 K; D, 973 K. (1), LNF10 with $d=1.00$ mm; (2), LNF10 with $d=0.60$ mm; (3), LSNF10 with $d=1.00$ mm; (4), LSNF10 with $d=0.50$ mm; (5), LNF2CU10 with $d=1.00$ mm; (6), LNF2CU10 with $d=0.59$ mm.

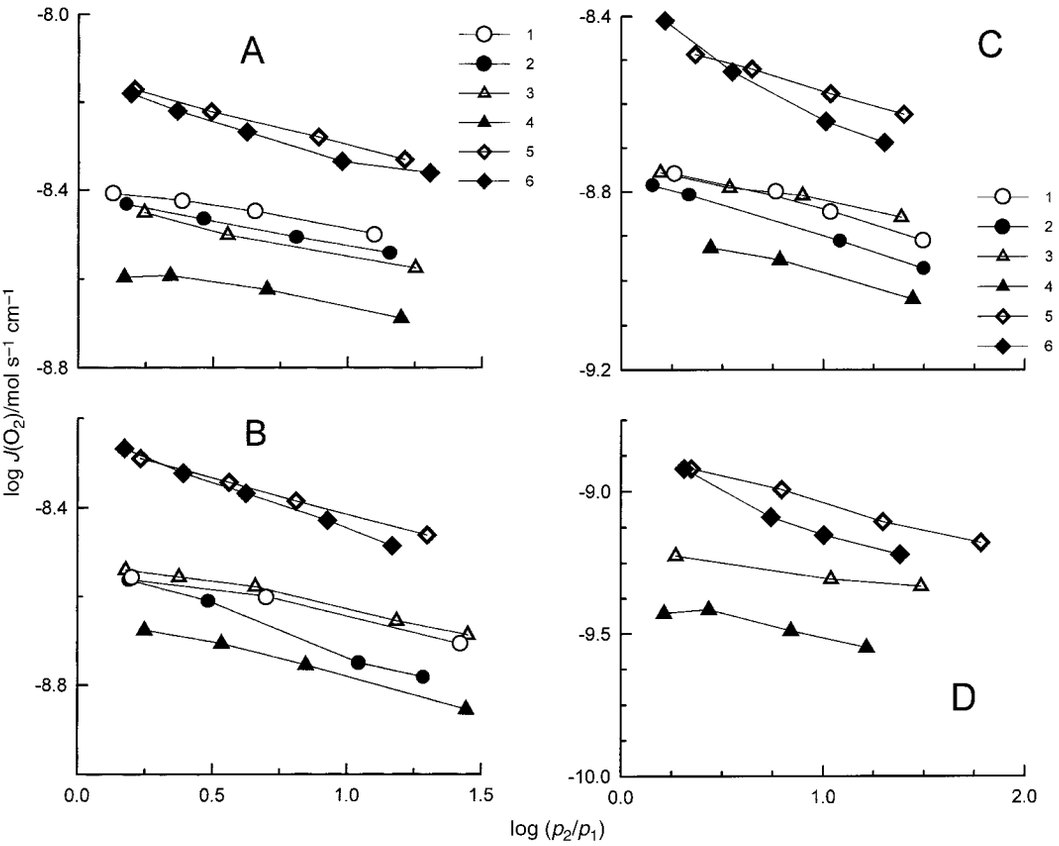

Fig. 3 Dependence of the oxygen permeability on the oxygen partial pressure gradient at: A, 1173 K; B, 1123 K; C, 1073 K; D, 973 K. (1), LNF10 with $d=1.00$ mm; (2), LNF10 with $d=0.60$ mm; (3), LSNF10 with $d=1.00$ mm; (4), LSNF10 with $d=0.50$ mm; (5), LNF2CU10 with $d=1.00$ mm; (6), LNF2CU10 with $d=0.59$ mm.

moderate oxygen chemical potential gradients ($p_1 > 0.05$ atm), the permeation flux through this membrane was close to the flux through the LNF10 membrane without an activating layer (Fig. 4). Further increase in the oxygen pressure gradient resulted in a higher oxygen permeability for the membrane with the activated feed-side, as compared to the unmodified membrane.

Attempts to modify the surface of the Fe-doped $La_2NiO_{4+\delta}$ ceramics by applying porous oxide layers of the same composition onto the membrane surface, in order to enlarge the specific surface area, failed. This was due to the excessively high temperatures required to achieve the necessary mechanical strength in the surface layers. For $SrCo_{0.8}Fe_{0.2}O_{3-\delta}$ (SCFO) ceramics, depositing porous SCFO layers with subsequent annealing at 1220–1330 K was reported to result in an enhancement of approximately 50% in the oxygen permeation flux.[32] In the case of iron-doped lanthanum nickelate membranes, however, temperatures as high as 1650–1700 K were necessary to prepare a mechanically strong layer from the powder with a particle size below 20 μm. After annealing the ceramics with such layers, the LNF10 and LSNF10 membranes demonstrated lower permeation fluxes with respect to the unmodified samples. This is because additional sintering of particles in the porous layers leads to a decrease of the effective surface area and an increase in the effective thickness of the membranes. Analogous results were obtained for porous cermet layers consisting of highly dispersed metallic silver and the doped nickelate powders. In this case, the mechanically strong layers could be prepared at significantly lower temperatures (*ca.* 1170–1420 K), but their catalytic activity was insufficient. As an example, Fig. 4 shows permeation fluxes through an LSNF10 membrane, the permeate-side surface of which was coated with a cermet of Ag (50 wt%) and LSNF10 (50 wt%). The sheet density of this porous cermet layer was approximately 10 mg cm^{-2}, similar to the previously mentioned mixture of platinum and praseodymium oxide (curve 2 in Fig. 4). Deposition of a Ag/LSNF10 cermet layer was found to decrease the permeation flux through LSNF10 ceramics due to both partial blocking of the membrane surface and increasing effective thickness.

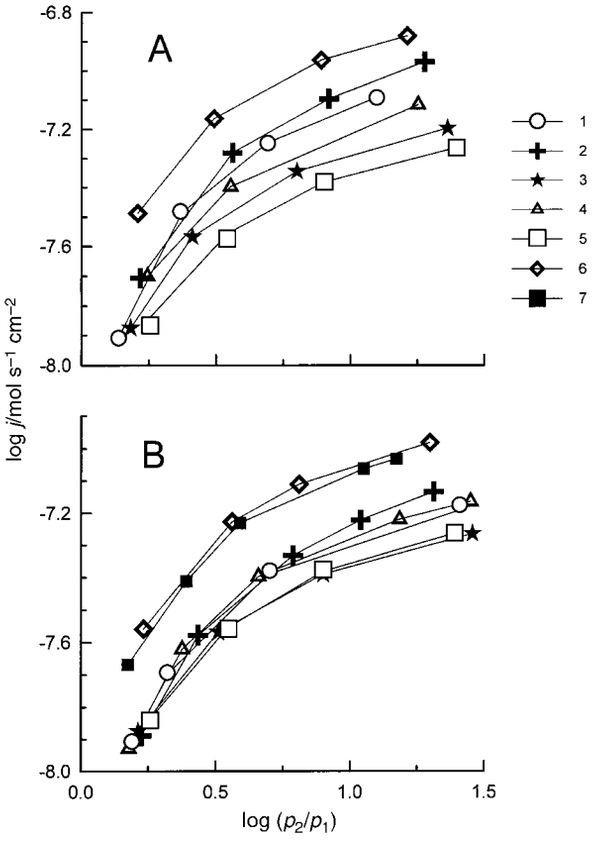

Fig. 4 Dependence of the oxygen permeation flux density on the oxygen partial pressure gradient at 1173 K (A) and 1123 K (B): (1) and (2), LNF10; (3), LSNF2; (4) and (5), LSNF10; (6), LNF2CU10; (7), LNF2. Curve 2 corresponds to the LNF10 membrane with a layer of platinum and praseodymium oxide deposited onto the feed-side surface. Curve 5 corresponds to the LSNF10 membrane with a layer of silver and LSNF10 powder applied onto the permeate-side surface. The thickness of all the ceramics was 1.00 ± 0.01 mm.

Comments on the oxygen transport mechanism

When analysing oxygen transport in the $La_2NiO_{4+\delta}$-based ceramics as a function of membrane cationic composition, one should take into consideration the data on $La_2CuO_{4+\delta}$ properties since they are closely related to those of lanthanum nickelate. At oxygen pressures of 0.21–1.0 atm, the lanthanum cuprate phase also exhibits oxygen hyperstoichiometry associated with incorporation of interstitial oxygen into the rock-salt layers of the K_2NiF_4 lattice,[12,33] but the δ values typical for $La_2CuO_{4+\delta}$ are lower than the oxygen nonstoichiometry of lanthanum nickelate.[7–10,13] The oxygen diffusivity along the perovskite layers of the $La_2CuO_{4+\delta}$ lattice was found to be considerably higher than along the *c* direction, through sequential NaCl–perovskite–NaCl-type layers.[34] Neglecting the oxygen hyperstoichiometry of lanthanum cuprate, oxygen diffusion in $La_2CuO_{4+\delta}$ and $La_{2-x}Sr_xCuO_{4+\delta}$ solid solutions was assumed to occur *via* a vacancy mechanism.[34,35] This assumption was based on experimental results showing a slight increase of the oxygen diffusion coefficient with strontium concentration in $La_{2-x}Sr_xCuO_{4\pm\delta}$ ($x = 0$–0.03), whereas further increase of x in the range 0.07 to 0.20 leads to a dramatic decrease in the oxygen diffusivity.[34,35] This behaviour was attributed to ordering of the oxygen sublattice[34] or immobilization of oxygen vacancies as a result of $2Sr_{La}' - V_O^{\cdot\cdot}$ clusters.[35] On the other hand, the migration energy values for oxygen vacancies and interstitial oxygen ions in tetragonal $La_2CuO_{4+\delta}$ were calculated to be similar and relatively low.[36] The calculations also showed an appreciable anisotropy in the migration energies in and out of the CuO_2 planes as well as a low probability for defect association between strontium ions and oxygen vacancies.[36,37] Our previous results on the $La_2Cu_{1-x}Co_xO_{4+\delta}$ solid solutions[27] demonstrated that both oxygen hyperstoichiometry and oxygen ionic conductivity in this system increase with partial substitution of copper with cobalt, indicating a participation of interstitial oxygen in the oxygen transport processes. Transference of oxygen to the rock salt interstices with formation of oxygen vacancies in the perovkite layers of the K_2NiF_4 lattice (intrinsic Frenkel defect formation) was suggested as a possible mechanism.[27]

As for $La_2CuO_{4+\delta}$-based materials, the results obtained on the doped $La_2NiO_{4+\delta}$ ceramics indicate that the oxygen ion conduction mechanism in nickelates is much more complex than simple hopping of oxygen ions between neighbouring vacancies. At temperatures above 1120 K, the oxygen permeability of the studied oxides was found to decrease in the sequence LNF2CU10 ≈ LNF2 > LSNF10 ≈ LNF10 > LSNF2 (Fig. 4). At 1073 K, the permeation fluxes through LSNF10, LNF10 and LSNF2 membranes are similar to each other, whereas the composition dependence of the permeability changes to LNF2CU10 > LNF2 > LSNF2 > LSNF10 > LNF10 with decreasing temperature down to 973 K (Fig. 5). No correlation between oxygen permeability and electronic conductivity was found.

The observed behaviour may be qualitatively explained in terms of two contributions to the total ionic conductivity

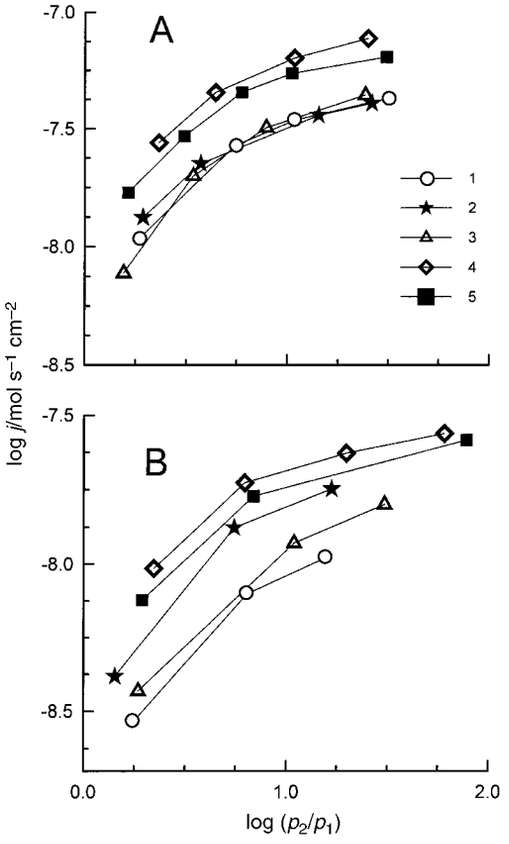

Fig. 5 Dependence of the oxygen permeation flux density on the oxygen partial pressure gradient at 1073 K (A) and 973 K (B): (1), LNF10; (2), LSNF2; (3), LSNF10; (4), LNF2CU10; (5), LNF2. The thickness of all the ceramics was 1.00 ± 0.01 mm.

of the nickelates: ionic conduction in the perovskite layers by the vacancy mechanism and migration of oxygen interstitials:

$$\sigma_o = \sigma_{ov} + \sigma_{oi} \quad (4)$$

where the indices 'v' and 'i' refer to the diffusion of oxygen vacancies and interstitials, respectively. Since the concentration of oxygen vacancies in the perovskite layers of the nickelates is much lower in comparison to that of the oxygen ions and the fraction of occupied interstices is also relatively low, the partial contributions to the total ionic conductivity under isothermal conditions can be expressed as:

$$\sigma_{ov} = K_{ov}[V_O^{\bullet\bullet}] \quad (5)$$

$$\sigma_{oi} = K_{oi}[O_i''] \quad (6)$$

where $[V_O^{\bullet\bullet}]$ and O_i'' are the concentrations of oxygen vacancies and interstitials, respectively, and K_{ov} and K_{oi} are the constants describing the temperature dependence. Notice that K_{ov} and K_{oi} represent functions of the bond energy of oxygen ions with the cation environment and geometrical parameters related to ion hopping.[38] Here, the activation energy for interstitial oxygen ion migration is assumed to be higher than that of ion transport *via* the vacancy mechanism.

As a rule, the energy of the oxygen anion to transition metal B cation bonds in the ABO_3 perovskite lattice decreases with increasing atomic number of the transition metal. Hence, one can anticipate a decrease in bond strength between oxygen ions and B-site cations in the perovskite layers of K_2NiF_4-type compounds in the sequence Fe–O > Ni–O ≈ Cu–O. According to the charge neutrality condition, incorporation of strontium into the lanthanum sublattice should result in either oxygen vacancy formation or a greater average oxidation state of the nickel cations:

$$[Sr_{La}'] = [Ni_{Ni}^{\bullet}] \quad (7)$$

or

$$[Sr_{La}'] = 2[V_O^{\bullet\bullet}] \quad (8)$$

In the case of strontium-doped lanthanum nickelate, both mechanisms take place; the first charge compensation mechanism expressed by eqn. (8) is more dominant at low strontium concentrations.[7,13] Note that a greater nickel cation oxidation state should increase the Ni–O bond strength.

One can, therefore, expect the following cation composition dependence for the parameters determining the vacancy controlled oxygen ionic transport: LNF2CU10 ≈ LNF2 > LSNF2 ≥ LNF10 > LSNF10 for K_{ov} and LSNF2 > LNF2CU10 ≈ LSNF10 ≥ LNF2 > LNF10 for $V_O^{\bullet\bullet}$. In contrast, the concentration of oxygen interstitials O_i'' should increase with iron content and decrease with doping by strontium: LNF10 > LNF2 ≥ LNF2CU10 ≥ LSNF10 > LSNF2. Hence, significant contributions from both oxygen vacancies in the perovskite layers and oxygen interstitials in the rock salt layers to the total ionic conductivity may be anticipated for LNF2 and LNF2CU10. For LNF10 and LSNF10, the oxygen interstitial diffusion is assumed to be predominant, whereas the oxygen vacancy contribution is higher for LSNF10 than that for LNF10. Finally, the ionic conductivity by the vacancy mechanism in LSNF2 ceramics is assumed to significantly exceed the interstitial migration contribution.

These assumptions are in qualitative agreement with the experimental data on the $La_2NiO_{4+\delta}$-based solid solutions (Fig. 4 and 5). Indeed, LNF2 and LNF2CU10 ceramics were found to exhibit the highest permeation fluxes with respect to other studied materials. The oxygen permeability of LNF10 ceramics at 1120–1170 K exceeds that of LSNF2, whereas reducing the temperature leads to decreasing permeability in the sequence LSNF2 > LSNF10 > LNF10, caused by the increasing role of diffusion *via* the vacancy mechanism with decreasing temperature.

One should also make a final remark concerning the possibly important role of the ceramic microstructure on oxygen transport in the oxides with the K_2NiF_4-type structure. In previous work,[39] preparation conditions and ceramic microstructure have been shown to have a significant effect on the oxygen transport in polycrystalline $LaCoO_{3-\delta}$. In particular, it has been found that an increase in sintering temperature leads to a change in the sintering mechanism and a drastic decrease of the grain boundary resistance to ionic transport in lanthanum cobaltite.[29] These results agree with data from Kilner *et al.*[40] which showed that the oxygen diffusion coefficient in grain boundaries of $La_{0.6}Sr_{0.4}Fe_{0.8}Co_{0.2}O_{3-\delta}$ ceramics exceeds the oxygen diffusivity in the grain bulk at 380–510 K by a factor of 10^5–10^3. In the case of LNF2CU10, the observed positive effect of doping with copper on the ionic conductivity can be partly attributed to a grain boundary contribution to oxygen transport. Since copper-containing oxides possess, as a rule, a relatively low melting point, sintering at lower temperatures in comparison with other nickelates was necessary to obtain gas-tight LNF2CU10 ceramics. A high copper content at the grain boundaries of sintered LNF2CU10 samples was observed by the micro-XFA technique, indicating a liquid-phase assisted sintering mechanism. Such a microstructure may influence, in agreement with our observations, the ion transport properties. The sintering processes, determining the microstructure and composition of the ceramic grain boundaries, were found to affect oxygen permeation through the $La_2NiO_{4+\delta}$-based ceramics to a considerable extent. In particular, increasing sintering temperature in the case of LSNF10 was shown to decrease the

permeation fluxes by a factor of 2–3. A detailed investigation of this effect is now in progress.

Conclusions

The solid solutions $La_2Ni_{1-x}Fe_xO_{4+\delta}$ ($x=0.02$ and 0.10), $La_{1.9}Sr_{0.1}Ni_{1-x}Fe_xO_{4+\delta}$ ($x=0.02$ and 0.10) and $La_2Ni_{0.88}Fe_{0.02}Cu_{0.10}O_{4+\delta}$ with the tetragonal K_2NiF_4-type structure were prepared by a standard ceramic route. The oxygen permeability, electrical conductivity and thermal expansion of the $La_2NiO_{4+\delta}$-based oxides were studied. The electronic conductivity of the solid solutions based on lanthanum nickelate increases with increasing strontium content and decreases when nickel is substituted by copper cations. For ceramic membrane thicknesses below 1.5 mm, oxygen permeation through dense nickelate ceramics is limited by both bulk ionic conductivity and surface exchange rates at the oxide/gas boundaries. The surface exchange limitations increased with decreasing oxygen pressure at the membrane permeate side and with decreasing temperature. Applying porous cermet layers of dispersed platinum and praseodymium oxide onto the membrane surface resulted in enhanced permeation fluxes. The maximum oxygen permeability in the temperature range 970–1170 K was found for the $La_2Ni_{0.98}Fe_{0.02}O_{4+\delta}$ and $La_2Ni_{0.88}Fe_{0.02}Cu_{0.10}O_{4+\delta}$ ceramics. Both a vacancy mechanism and an oxygen interstitial migration contribute significantly to the ionic conduction. Thermal expansion coefficients of the ceramic materials were calculated from the dilatometric data to vary in the range $(10.5–13.2)\times10^{-6}\ K^{-1}$ at 300–1100 K.

Acknowledgements

This work was partially supported by the Belarus Foundation for Basic Research, the FCT (PRAXIS, Portugal) and the company B-2 Limited.

References

1 B. C. H. Steele, in *Proc. 1st European SOFC Forum*, ed. U. Bossel, Lucerne, 1994, vol. 1, p. 375.
2 J. Mizusaki, *Solid State Ionics*, 1992, **52**, 79.
3 H. J. M. Bouwmeester and A. J. Burgraaf, in *Fundamentals of Inorganic Membrane Science and Technology*, ed. A. J. Burgraaf and L. Cot, Elsevier, Amsterdam, 1996, p. 435.
4 T. J. Mazanec, in *Ceramic Membranes I*, ed. H. U. Anderson, A. C. Krandhar and M. Liu, Electrochemical Society, Pennington, NJ, 1995, p. 16.
5 R. T. Baker, B. Charbage and F. M. B. Marques, *J. Electrochem. Soc.*, 1997, **144**, 3130.
6 V. V. Kharton, E. N. Naumovich and A. V. Nikolaev, *J. Membr. Sci.*, 1996, **111**, 149.
7 Y. Takeda, R. Kanno, M. Sakano, O. Yamamoto, M. Takano, Y. Bando, H. Akinada, K. Takita and J. B. Goodenough, *Mater. Res. Bull.*, 1990, **25**, 293.
8 A. Demourgues, P. Dordor, J.-P. Doumerk, J.-C. Grenier, E. Marquestaut, M. Pouchard, A. Villesuzanne and A. Wattiaux, *J. Solid State Chem.*, 1996, **124**, 1999.
9 D. E. Rice and D. J. Buttrey, *J. Solid State Chem.*, 1993, **105**, 197.
10 H. Tamura, A. Hayashi and Y. Ueda, *Physica C*, 1993, **216**, 83.
11 M. T. Fernandez-Diaz, J. L. Martinez and J. Rodriguez-Carvajal, *Solid State Ionics*, 1993, **63–65**, 902.
12 H. Kanai, J. Mizusaki, H. Tagawa, S. Hoshiyama, K. Hirano, K. Fujita, M. Tezuka and T. Hashimoto, *J. Solid State Chem.*, 1997, **131**, 150.
13 V. V. Vashook, S. P. Tolochko, I. I. Yushkevich, L. V. Makhnach, I. F. Kononyuk, H. Altenburg, J. Hauck and H. Ullmann, *Solid State Ionics*, 1998, **110**, 245.
14 S. P. Tolochko, L. V. Makhnach, I. F. Kononyuk and V. V. Vashook, *Zh. Neorg. Khim.*, 1994, **39**, 1092 (in Russian).
15 F. Gervais, P. Odier and Y. Nigara, *Solid State Commun.*, 1985, **56**, 371.
16 I. F. Kononyuk, N. G. Surmach and L. V. Makhnach, *Neorg. Mater.*, 1982, **18**, 1222 (in Russian).
17 C. N. R. Rao, P. Ganguly, K. K. Singh and R. A. Mohan Ram, *J. Solid State Chem.*, 1988, **72**, 14.
18 J. F. DiCarlo, I. Yazdi, S. Bhavaraju and A. J. Jacobson, *Chem. Mater.*, 1993, **5**, 1692.
19 V. V. Vashook, M. V. Zinkevich, L. V. Makhnach, S. P. Tolochko and I. F. Kononyuk, *Neorg. Mater.*, 1998, **34**, 622 (in Russian).
20 V. V. Kharton, Li Shuangbao, A. V. Kovalevsky and E. N. Naumovich, *Solid State Ionics*, 1997, **96**, 141.
21 V. V. Kharton, Li Shuangbao, A. V. Kovalevsky, A. P. Viskup, E. N. Naumovich and A. A. Tonoyan, *Mater. Chem. Phys.*, 1998, **53**, 6.
22 V. V. Kharton, V. N. Tikhonovich, Li Shuangbao, E. N. Naumovich, A. V. Kovalevsky, A. P. Viskup, I. A. Bashmakov and A. A. Yaremchenko, *J. Electrochem. Soc.*, 1998, **145**, 1363.
23 V. V. Kharton, E. N. Naumovich, A. V. Kovalevsky, A. A. Yaremchenko, A. P. Viskup and P. F. Kerko, *J. Membr. Sci.*, 1999, in press.
24 V. V. Kharton, A. P. Viskup, E. N. Naumovich, A. A. Tonoyan and O. P. Reut, *Mater. Res. Bull.*, 1998, **33**, 1087.
25 H.-H. Moebius, in *Extend. Abstr. 37th Meet. ISE*, Vilnius, Lithuania, 1986, vol. 1, p. 136.
26 K. K. Singh, P. Ganguly and J. B. Goodenough, *J. Solid State Chem.*, 1984, **52**, 254.
27 D. M. Bochkov, V. V. Kharton, A. V. Kovalevsky, A. P. Viskup and E. N. Naumovich, *Solid State Ionics*, 1999, **120**, 281.
28 V. N. Tikhonovich, D. M. Bochkov, V. V. Kharton, E. N. Naumovich and A. P. Viskup, *Mater. Res. Bull.*, 1998, **33**, 89.
29 S. P. Tolochko, I. F. Kononyuk, S. F. Strelchik and E. A. Korzyuk, *Vesti AN BSSR*, 1984, **4**, 64 (in Russian).
30 V. N. Tikhonovich, V. V. Kharton, E. N. Naumovich and A. A. Savitsky, *Solid State Ionics*, 1998, **106**, 197.
31 V. V. Kharton, E. N. Naumovich and A. A. Vecher, *J. Solid State Electrochem.*, 1999, **3**, 61.
32 T. H. Lee, Y. L. Yang and A. J. Jacobson, in *Ceramic Membranes I*, ed. H. U. Anderson, A. C. Krandhar and M. Liu, Electrochemical Society, Pennington, NJ, 1995, p. 72.
33 J. D. Jorgensen, B. Dabrowski, S. Pei, D. G. Hinks, L. Soderholm, B. Morosin, J. E. Schirber, E. L. Venturini and D. S. Ginley, *Phys. Rev. B*, 1988, **38**, 11337.
34 E. J. Opila, H. L. Tuller, B. J. Wuensch and J. Maier, *J. Am. Ceram. Soc.*, 1993, **76**, 2363.
35 J. L. Routbort, S. J. Rothman, B. K. Flandermeyer, L. J. Nowicki and J. E. Baker, *J. Mater. Res.*, 1988, **3**, 116.
36 N. L. Allan and W. C. Mackrodt, *Philos. Mag. A*, 1991, **64**, 1129.
37 N. L. Allan and W. C. Mackrodt, *Philos. Mag. A*, 1988, **58**, 555.
38 V. N. Chebotin, *Physical Chemistry of Solids*, Khimiya, Moscow, 1982 (in Russian).
39 V. V. Kharton, E. N. Naumovich, A. V. Kovalevsky, A. P. Viskup, A. A. Yaremchenko and I. A. Bashmakov, *Solid State Ionics*, 1999, in press.
40 S. J. Benson, R. J. Chater and J. A. Kilner, in *Ionic and Mixed Conducting Ceramics III*, ed. T. A. Ramanarayanan, Electrochemical Society, Pennington, NJ, 1998, p. 596.

Paper 9/03276B